http://ansinet.com/itj

ITJ

ISSN 1812-5638

INFORMATION TECHNOLOGY JOURNAL

ANSInet
Asian Network for Scientific Information
308 Lasani Town, Sargodha Road, Faisalabad - Pakistan

Information Technology Journal 10 (12): 2446-2451, 2011
ISSN 1812-5638 / DOI: 10.3923/itj.2011.2446.2451

Simulation of Heating Cell in a New Integrated Solar Plate-fin Desalination Unit by Fluent

[1,2]Shu Xu, [2]Xiang Ling and [2]Hao Peng
[1]School of Mechanical Engineering, Huaihai Institute of Technology, Lianyungang, 222005, China
[2]School of Mechanical and Power Engineering, Nanjing University of Technology, Nanjing, 210009, China

Abstract: Supply of adequate quantities of fresh potable water is one of the most serious problems confronting human. To resolve this crisis, solar distillation is a typical process where solar energy is used to distil fresh water from saline or brackish water for drinking purposes and other applications. It is generally classified into passive and active distillation systems. This study proposed a new solar plate-fin distillation system that was designed to increase the productivity and improve the efficiency of the solar plate-fin still. The solar still worked by virtue of the higher evaporation rate under vacuum conditions. A mathematical model was developed and used to optimize the design of the heating cell. Also, presented and discussed in a detail description of local and average heat transfer characteristics of the serrated fins. Results indicated different structure of heating cell has a significant effect on the characters of the new solar plate-fin desalination unit.

Key words: Solar desalination, solar plate-fin still, numerical simulations

INTRODUCTION

The demand for a steady, economical supply of water is constantly increasing all around the world and supply often does not equal the present needs. A very small fraction, about 0.3%, of the available water resources is available as fresh water (Delyannis and Belessiotis, 2001). This problem will become more difficult to solve in the future. Desalination is an excellent solution to the problem, provided that there are sufficient quantities of salt water to meet the needs of the inhabitants. There are many methods of converting brackish water into potable water. Among the processes which are now commercially employed, the distillation of brackish or seawaters is considered to be one of the simplest and widely adopted technique for converting salted water to fresh water.

But desalination processes consume significant amounts of energy. The energy consumption for desalination will continue to rise and hence the amount of conventional hydrocarbon fuels required will substantially go up. In terms of oil consumption, it is estimated that about 203 million tons of oil per year is required to produce 22 million m^3 per day of desalinated water (Kalogirou, 2005). The usage of fossil fuels continues to pollute the environment and adds to the cause of global warming. These technologies thus contribute indirectly to greenhouse gas emissions and are not sustainable. While solar stills are driven by solar energy, they do not suffer from these shortcomings. Desalination using solar energy is increasingly becoming an attractive option. Therefore, solar desalination can be a suitable alternative, provided efficient technologies are developed to utilize the solar energy in a cost-effective way. Thermal solar energy water desalination has proved to be one of practical methods to produce fresh water from saline water (Al-Kharabsheh and Goswami, 2003).

Solar energy can be used to produce fresh water directly in a solar still or indirectly where the thermal energy from a solar energy system is supplied to a desalination unit. A number of efforts have been made to improvement in the still's performance (Kunze, 2001; Schwarzer *et al*., 2001). Theoretical studies on a multi-stage tray solar still operating in a steady state regime were performed by Adhikari *et al*. (1995). The authors presented a mathematical model of a three-stage unit and their theoretical results were validated experimentally using an electric heater energy source. Eames *et al*. (2007) described the results of theoretical and experimental investigations on a small-scale solar powered barometric desalination system. Zejli *et al*. (2004) designed a combination of a MED system with an open cycle adsorptive heat pump using internal heat recovery. The heat transfer fluid flowing through tubes in the adsorbent beds is heated up by a parabolic trough collector. Theoretical modeling was done and variation of energy consumption and performance ratio with the number of effects is shown. Performance ratio is defined as the ratio of water produced to the required heat input. Al-Hawaj and Darwish (1994) coupled MED with a solar pond. A numerical modeling of a multi-stage solar still with an expansion nozzle and heat recovery for steady state conditions was undertaken by Jubran *et al*. (2000) . Other

Corresponding Author: Shu Xu, School of Mechanical Engineering, Huaihai Institute of Technology, Lianyungang, 222005, China

researchers (Bemporad, 1995; Jubran *et al*., 2000) have investigated the concept of evaporation at low temperatures under vacuum conditions and reported good improvement in the system performance. However, they used vacuum pumps which require additional energy input to the system. The disadvantages of basin solar stills include their relatively low performance due to excessive heat losses to the ambient surrounding, their generally low thermal efficiency and progressing reduction in efficiency over the exploitation period because of the scaling and accumulation of salt impurities (Abakr and Ismail, 2005). The maximum thermal efficiency of basin solar stills is usually around 25%, with an average distillate output capacity of 1.5-3.0 kg/m/day.

This study proposed a new solar plate-fin distillation system that was designed to increase the productivity and improve the efficiency of the solar plate-fin still. The solar still worked by virtue of the higher evaporation rate under vacuum conditions. Serrated fins are used in the heating cell, thermal fluid flow through serrated fins in different directions. A mathematical model was developed and used to optimize the design of the heating cell. Also presented and discussed in a detail description of local and average heat transfer characteristics of the serrated fins. Results indicated different structure of heating cell has a significant effect on the characters of the new solar plate-fin desalination unit.

PRESENTATION OF SINGLE-EFFECT SOLAR PLATE-FIN DESALINATION UNIT

The desalination unit consists of a solar unit which provides the thermal energy and a desalination module that uses a new integrated plate-fin desalination unit to treat the brackish water. The new integrated plate-fin desalination unit is brazed with 316 L stainless steel and it has good sealing.

The desalination unit is composed of the evaporation/condensation cell that is, respectively heated and cooled by the heating and cooling cells. The heating of the evaporation cell is ensured by hot water (80°C) flowing upward along heating cells (Fig. 1). The hot water is produced thanks to the solar unit. The cooling of the condensation cell is also ensured by cold seawater flowing in the same way. The preheated salted water enters on top of the evaporation cell and water is distributed all along the plate-fin thanks to a distribution system. Brine and distilled water flow by gravity and are collected at the bottom of the vapor-condensation cell.

Serrated fins are used in integrated plate-fin desalination unit. They have a high degree of surface compactness and act to interrupt the flow and create a series of thin boundary layers which lead to enhance the overall heat transfer rate. In heating cell ,two different types serrated fins can be used .One is Transverse Flow Direction (TFD). In this situation, the fluid flow is perpendicular to the fin surface, as shown in Fig. 2. The other kind is Longitudinal Flow Direction (LFD) in which condition the fluid flows parallel to the fin surface, as shown in Fig. 3. In this study, taking heating water as working fluid, the heat transfer Colburn factor j and the friction factor f characteristics of the LFD type and TFD type serrated fins in heating cell are investigated both numerically.

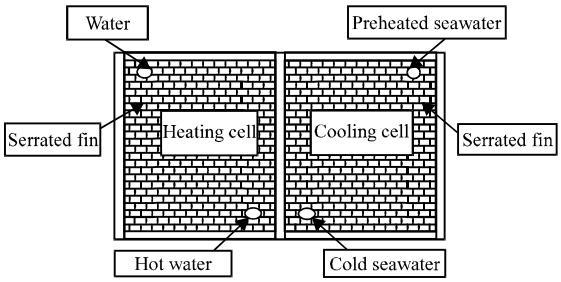

Fig. 1: Scheme of heating cell and cooling cell

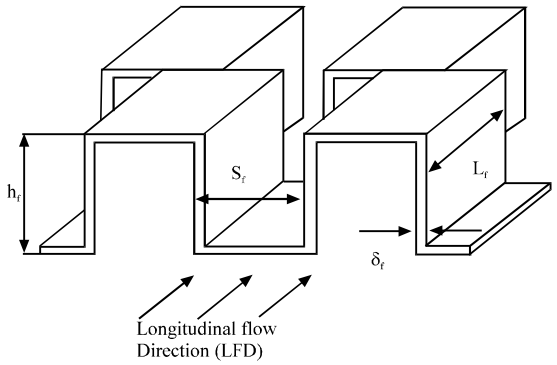

Fig. 2: Longitudinal Flow Direction (LFD) for serrated fins

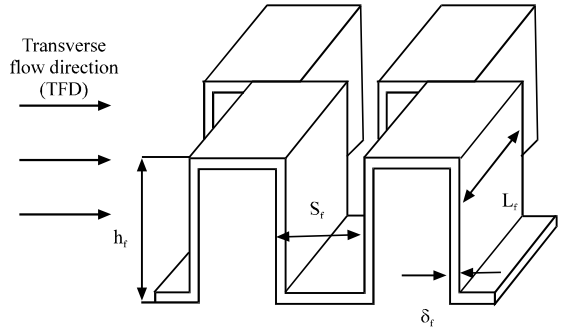

Fig. 3: Transverse Flow Direction (TFD) for serrated fins

The typical serrated fin structure is shown in Fig. 2 and 3. Their major surface geometries are described by the fin height h_f, fin space s_f, fin thickness δ_f, fin length L_f. The fins are uniformly offset by half the fin spacing and designed to be of equal size and shape to maintain the geometric periodicity. For the present study, the experimental and numerical serrated fin schemes are chosen in Table 1.

MODELING APPROACH

Conservation equations: Some simplifying assumptions are required before applying the conventional flow equations and energy equations to model the flow and heat transfer process in the serrated fins. The major assumptions are:

- The water flow through fins is characterized by small hydraulic diameter and low Reynolds number under practical work conditions, so the flow is laminar
- The thermo-physical properties are temperature independent
- The flow inside the serrated fins is considered to be incompressible and steady
- Thermal radiation and nature convection are neglected
- Ideal surfaces, i.e., no burrs or scarped edges, perfect contact at channel walls and uniform surface dimensions throughout the array

Based on these approximations, the governing equations used to describe the fluid flow and heat transfer in the serrated fins are established. First consider the fluid area. The mass, momentum and energy equations for the three dimensional models are as follows:

Continuity equation:

$$\rho_l \frac{\partial u_i}{\partial x_i} = 0 \quad (1)$$

Momentum equation:

$$\frac{\partial}{\partial x_j}(u_i u_j) = \frac{\mu_l}{\rho_l}\nabla^2(u_i) - \frac{1}{\rho_l}\frac{\partial p}{\partial x_i} \quad (2)$$

Energy equation:

$$\rho_l \frac{\partial T_l}{\partial t} = \frac{\lambda_l}{c_p}\frac{\partial}{\partial x_j}\left(\frac{\partial T_l}{\partial x_j}\right) + S_T \quad (3)$$

For the solid area, the energy equation is written as:

$$\lambda_w \frac{\partial}{\partial x_j}\left(\frac{\partial T_w}{\partial x_j}\right) = 0 \quad (4)$$

To form a closed set of equations, additional relations are required including the boundary conditions and transport properties of the water (density, heat capacity, heat conductivity, viscosity).

3D meshes of model: Figure 2 and 4 are the schemes of LFD and TFD type serrated fins, respectively. These two models are similar in structure except for the flow direction. They consist of two solid separating boards, several fins units and two symmetry walls. In order to remove the entrance effects inside the flow region, the fins are in the center of the computational domain at the same distance from the inlet and outlet parts.

The hexahedral mesh is used for the present computations, as illustrated in Fig. 4 and 5. The grid independence is checked using two different mesh sizes. For coarse mesh, cell size equal to fin thickness is used and for fine mesh, cell size is half of the fin thickness. It is found that the variation in solutions is within 2-3%.

Table 1: Dimension of the serrated fins

Parameter	h_f (mm)	s_f (mm)	δ_f (mm)	L_f (mm)	Flow direction
1	6	4	0.2	5	LFD
2	6	4	0.2	5	TFD

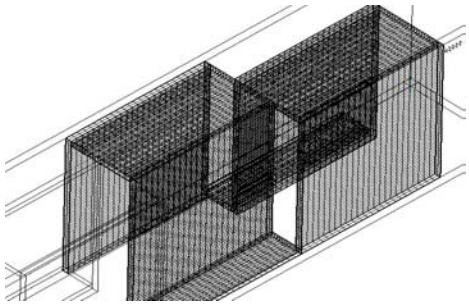

Fig. 4: Typical mesh of the computational domain (LFD)

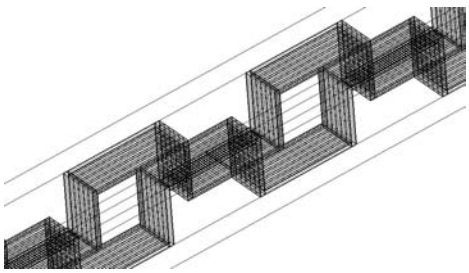

Fig. 5: Typical mesh of the computational domain (TFD)

The grid-generation procedure is suitably modified in order to decrease the temperature gradients at the near-wall region. This computational action, that allowed the use of the medium grid for large zones, was successful as represented a good compromise between accurate results and available calculation resources.

Boundary conditions: As shown in Fig. 4 and 5, at the inlet, uniform profiles for all the variables were employed:

$$U_i = u_{hs,i} \tag{5}$$

$$T_i = T_{hs,i} \tag{6}$$

where, Ui is normal water velocity perpendicular to the inlet, Ti is water inlet temperature. The values of water velocities and temperatures are determined by the available experimental data.

On the interface between fluid and solid, the matching heat flux boundary condition is given below:

$$-\lambda_w \frac{\partial T_w}{\partial n}\bigg|_\Gamma = -\lambda_l \frac{\partial T_l}{\partial n}\bigg|_\Gamma \tag{7}$$

A non-slip boundary condition was imposed at the tube wall and the outlet boundary conditions were set up as a pressure outlet boundary instead of as an outflow boundary to avoid difficulties with backflow.

The heat transfer performance and pressure drop of serrated fins for a given geometric and flow conditions can be characterized by a Colburn factor j and a friction factor f, respectively. And the flow conditions can be characterized by Reynolds number which can be calculated in terms of dimension parameters such as fin pitch, fin height, fin thickness etc.

DETERMINATION OF PERFORMANCE PARAMETERS

In integrated plate-fin desalination unit, The Colburn factor j and friction factor f can be defined as:

$$j = St\, Pr^{2/3} \tag{8}$$

$$f\cdot\left(\frac{4L}{D_e}\frac{\rho_i}{\rho_m}\right) = 2\frac{\Delta P}{\rho_m u^2} - [(K_c + 1 - \sigma^2) + (1 - \sigma^2 - K_e)\cdot\frac{\rho_i}{\rho_o} + 2\left(\frac{\rho_i}{\rho_o} - 1\right)] \tag{9}$$

While the Prandtl number is:

$$Pr = \frac{\mu c_p}{\lambda} \tag{10}$$

The Stanton number can be evaluated by solving Eq. 11:

$$St = \frac{q_w}{c_p G(T_m - T_w)} \tag{11}$$

where, q_w is the mean heat flux density, G is the mass flux and Tm is the average temperature between the inlet and outlet temperatures:

$$q_w = \frac{Q}{A_c} \tag{12}$$

$$T_m = \frac{T_i + T_o}{2} \tag{13}$$

The Reynolds number is defined in terms of hydraulic diameter De:

$$Re = \frac{uD_e}{\nu} \tag{14}$$

$$D_e = \frac{2(h_f - \delta_f)(s_f - \delta_f)}{(h_f - \delta_f) + (s_f - \delta_f)} \tag{15}$$

RESULT AND DISCUSSION

Numerical simulation for LFD type serrated fins: The first part of the simulation works are carried out using a detailed schematization of the small periodic units of LFD type serrated fins at the water side in the integrated plate-fin desalination unit. The flow is considered a laminar flow and the standard wall function is used to predict the near wall region flow.

Take sample No. 1 for example which has a fin height of 6.0 mm, fin pitch of 4.0 mm, fin thickness of 0.2 mm, effective length of 5 mm and hydraulic diameter of 4.06 mm. For a given water inlet temperature (303 K) and water inlet velocity (0.3 m sec^{-1}) and the temperature of the clapboards is 353 K. The corresponding Reynolds value is 938 which calculated at the inlet section. Figure 6 shows the velocity distributions on a horizontal and on a vertical section. In Fig. 6 some zones with water velocity and others of stagnation due to the fins can be observed. Figure 7 shows the temperature distributions on a horizontal and on a vertical section it shows the most relevant temperature trends on the walls and in the flow on vertical parts of fins and in the center of the computational domain. From Fig. 10, it is clear that the temperature of the fluid is originally uniform at the channel inlet and changes due to the development of the thermal boundary layer, while the temperature variation in the near wall region is much higher than in the fluid flow core.

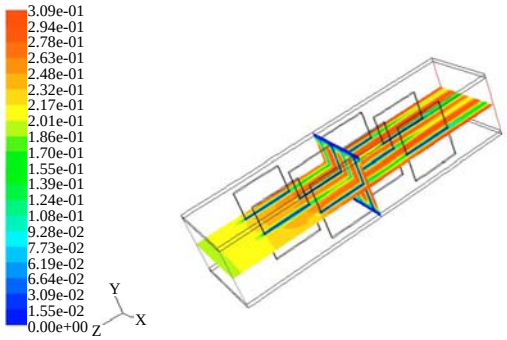

Fig. 6: Water velocity distributions in the numerical model (60JC4002/LFD)

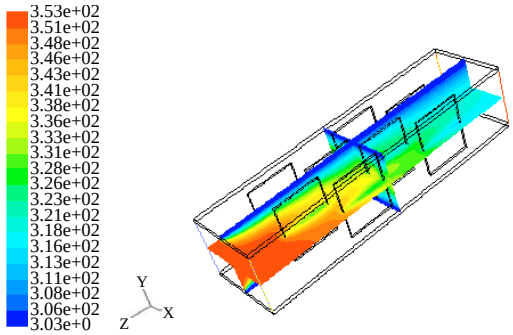

Fig. 7: Water temperature distributions in the numerical model (60JC4002/LFD)

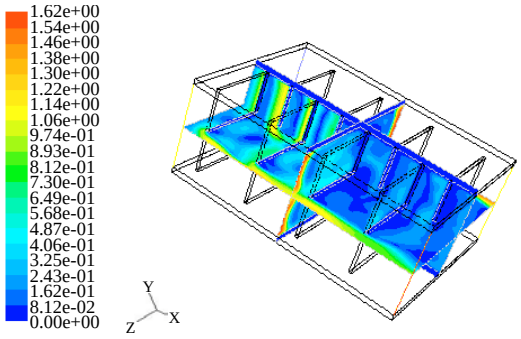

Fig. 8: Water velocity distributions in the numerical model (60JC4002/TFD)

Numerical simulation for TFD type serrated fins: The second part of the simulation work involved 3D-simulations of the heat and flow characteristics for transverse flow through the serrated fins. In this part, sample No. 2 was considered. Figure 8 shows the velocity and temperature distributions on a horizontal and on a vertical section accorded with the corresponding

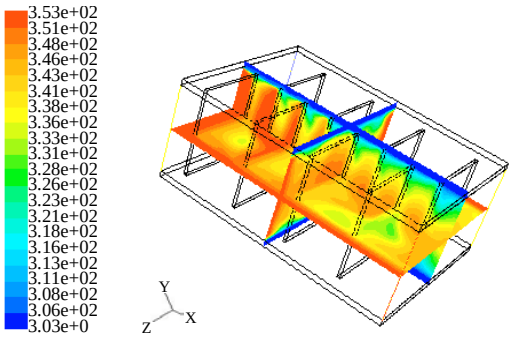

Fig. 9: Water temperature distributions in the numerical model (60JC4002/TFD)

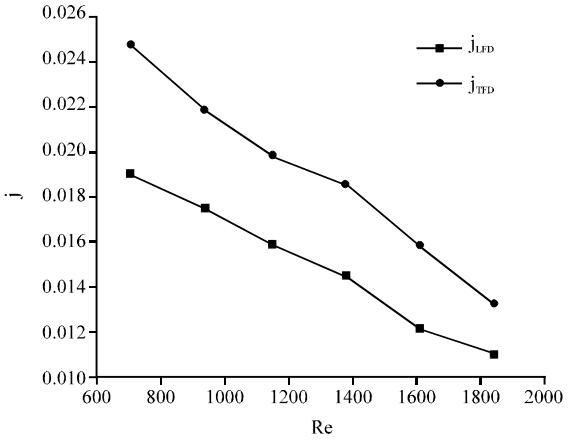

Fig. 10: Comparison between the numerical calculations for j_{LFD} and j_{TFD}

experiments for the Reynolds number Re = 1377. Figure 8 shows the front view of the flow configuration. This flow field is neither similar nor dissimilar to the LFD type flows. It can be seen that in the TFD type serrated fin's geometries, fluid flows across a side or vertical surface but since the flow is constrained by the channel walls, the fluid must flow around the obstacle. Actually, this movement provides enhancement of heat transfer coefficient by means of intensified the interrupted flow. And the trend for the temperature distributions of TFD type fins is similar to LFD type fins which the temperature gradient in the near wall region is much higher than in the center of fluid flow (Fig. 9).

Comparison between LFD type serrated fins and TFD type serrated fins: The overall Colburn factor j and the friction factor f were determined for the fin geometry used in the preceding computations, using equations given determination of performance para meter. Numerical computations were made for different water Reynolds

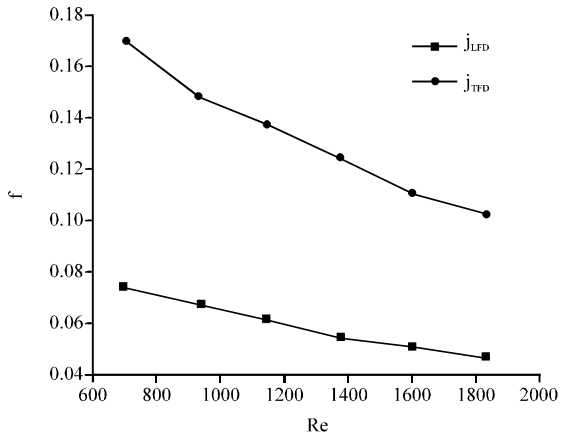

Fig. 11: Comparison between the numerical calculations for f_{LFD} and f_{TFD}

numbers. Figure 10-11 shows the comparison of Colburn factor j and friction factor f between the numerical simulations for the sample of LFD type serrated fin and the sample of TFD type serrated fins. From these figures, it can be seen that all the numerical calculation for j of LFD type serrated fin is 20-30% different from j of TFD type serrated fin while the numerical calculation for f of TFD type serrated fin is twice as much as f of LFD type serrated fin. The computed Colburn factor and friction factor have degressive slope for the increase of Reynolds number. From the Fig. 10-11, it can be found that the above-presented numerical method can be successfully predicted the thermal performance of LFD type serrated fins and TFD type serrated fins.

CONCLUSION

In this study, Numerical investigation of the heating cell is presented. Fluent software is used to simulate the simultaneous heat-mass of the heating cell. The heat transfer Colburn factor j and friction factor f of LFD type serrated fins and TFD type serrated fins in steel are investigated numerically. Also, presented and discussed is a detailed description of the local and average heat transfer characteristics of the fins, i.e., temperature distribution, velocity distribution. Key findings of this study are as follows: all the numerical calculation for j of LFD type serrated fin is 20-30% different from j of TFD type serrated fin while the numerical calculation for f of TFD type serrated fin is twice as much as f of LFD type serrated fin; The computed Colburn factor and friction factor have digressive slope for the increase of Reynolds number. The heat carrier fluid thermal resistance Rw is inversely proportional to the heating water Reynolds number. Therefore, properly choice of heating water velocity is imperative.

These results will be used to choose the best operating conditions for real seawater tests planned in Italy. These tests will allow us to complete the thermal study, particularly to evaluate the heat transfer coefficient between condensation and evaporation cells. It will then be possible to size an industrial unit.

REFERENCES

Abakr, Y.A. and A.F. Ismail, 2005. Theoretical and experimental investigation of a novel multistage evacuated solar still. J. Sol. Energy Eng., 127: 381-385.

Adhikari, R.S., A. Kumar and G.D. Sootha, 1995. Simulation studies on a multi-stage stacked tray solar still. Solar Energy, 54: 317-325.

Al-Hawaj, O. and M.A. Darwish, 1994. Performance characteristics of a multi effect solar pond desalting system in an arid environment. Desalination, 96: 3-10.

Al-Kharabsheh, S. and D.Y. Goswami, 2003. Analysis of an innovative water desalination system using low-grade solar heat. Desalination, 156: 323-332.

Bemporad, G.A., 1995. Basic hydrodynamic aspects of a solar energy based desalination process. Desalination, 54: 125-134.

Delyannis, E. and V. Belessiotis, 2001. Solar Energy and Desalination. In: Advances in Solar Energy: An Annual Review of Research and Development, Goswami, D.Y. (Ed.). Vol. 14, American Solar Energy Society, Boulder, Colorado, pp: 287-330.

Eames, I.W., G.G. Maidment and A.K. Lalzad, 2007. A theoretical and experimental investigation of a small-scale solar-powered barometric desalination system. Applied Thermal Eng., 27: 1951-1959.

Jubran, B.A., M.I. Ahmed, A.F. Ismail and Y.A. Abakar, 2000. Numerical modelling of a multi-stage solar still. Energy Convers. Manage., 41: 1107-1121.

Kalogirou, S.A., 2005. Seawater desalination using renewable energy sources. Progr. Energy Combust. Sci., 31: 242-281.

Kunze, H., 2001. A new approach to solar desalination for small and medium-size use in remote areas. Desalination, 139: 35-41.

Schwarzer, K., M.E. Vieira, C. Faber and C. Muller, 2001. Solar thermal desalination system with heat recovery. Desalination, 137: 23-29.

Zejli, D., R. Benchrifa, A. Bennouna and O.K. Bouhelal, 2004. A solar adsorption desalination device: First simulation results. Desalination, 168: 127-135.